Asian Journal of Chemistry; Vol. 36, No. 5 (2024), 1072-1088

ASIAN JOURNAL OF CHEMISTRY

https://doi.org/10.14233/ajchem.2024.31342

# *In silico* Analysis of 1,3,4-Oxadiazoles as Potential BCL-2 Inhibitor for Cancer Treatment

GANESH SONAWANE*, SHWETA SHARMA and RITU GILHOTRA

Gyan Vihar School of Pharmacy, Suresh Gyan Vihar University, Jaipur-302017, India

*Corresponding author: E-mail: gbsonawane8@gmail.com

*Received*: 4 February 2024; *Accepted*: 18 March 2024; *Published online*: 30 April 2024; AJC-21612

The possible efficacy of 1,3,4-oxadiazoles as B-cell lymphoma 2 (BCL-2) inhibitors for cancer treatment is investigated in this study using *in silico* approaches such as molecular docking, ADME and toxicity prediction. Molecular docking studies predict the binding affinities and binding modes of a series of 1,3,4-oxadiazole derivatives with the BCL-2 protein. The results revealed that the compounds with strong interactions and favourable binding modes, indicating their potential as BCL-2 inhibitors. An ADMET analysis assesses the pharmacokinetic properties and potential toxicity of the identified compounds. Parameters such as absorption, distribution, metabolism, excretion and toxicity (ADMET) were evaluated to predict the suitability of these 1,3,4-oxadiazoles as drug candidates for cancer therapy. The integration of molecular docking and ADMET analysis data led to the identification and prioritization of lead compounds with potent BCL-2 inhibitory activity and favourable pharmacokinetic profiles. This research contributes to the on-going efforts in drug discovery, emphasizing the potential of 1,3,4-oxadiazoles as a class of compounds with significant anticancer properties through BCL-2 inhibition.

**Keywords: 1,3,4-Oxadiazoles, Cancer, BCL-2, Molecular docking, ADMET analysis, ProTox-II.**

## INTRODUCTION

B-cell lymphoma 2 (BCL-2) is a pivotal regulator of apoptosis, a fundamental process in cellular homeostasis crucial for preventing the emergence of cancerous cells [1]. As a member of the BCL-2 protein family, BCL-2 plays a central role in modulating the permeability of the mitochondrial outer membrane, a critical step in the apoptotic pathway. The primary function of BCL-2 is to suppress apoptosis, thereby promoting cell survival. This is achieved by inhibiting the release of cytochrome c from the mitochondria into the cytoplasm, a process that, when activated, initiates a cascade of events leading to programmed cell death [2]. In cancer, the dysregulation of the apoptotic pathway, including alterations in BCL-2 expression, is frequently observed. Overexpression of BCL-2 can confer a survival advantage to cancer cells by preventing apoptosis, allowing for uncontrolled proliferation [3]. Consequently, BCL-2 has emerged as a promising therapeutic target in cancer treatment.

Strategies aimed at modulating BCL-2 activity, such as the development of small molecules like 1,3,4-oxadiazoles, offer potential avenues for innovative cancer therapies [4]. Understanding the molecular mechanisms underlying BCL-2 function and its interactions with potential inhibitors is essential for advancing targeted cancer therapy. Research efforts, including molecular docking studies, ADME and toxicity study, contribute to elucidating the therapeutic potential of compounds targeting BCL-2 [5]. Targeting the BCL-2 protein in cancer treatment has the potential to address critical challenges associated with cancer cell survival, resistance to therapies and the need for more selective and effective treatment options [6,7]. As research progresses, BCL-2 inhibition emerges as a promising avenue for developing novel and targeted therapeutic strategies in the fight against cancer [8-12]. The research on 1,3,4-oxadiazoles as potential BCL-2 inhibitors for cancer treatment provides promising insights, combining molecular docking studies with *in silico* ADMET analysis to identify compounds with strong binding affinities and favourable drug-like properties [13]. Novel approaches to drug discovery have been made possible by recent developments in computational biology, especially with regard to targeted cancer treatments. Modern techniques including molecular docking and ADMET analysis are used to find and assess potential anticancer medications [14,15]. In present study, virtually designed 1,3,4-oxadiazoles (Fig. 1) were subjected to various *in silico* analysis for screening and exploring their potential as BCL-2 inhibitors for anticancer activity.

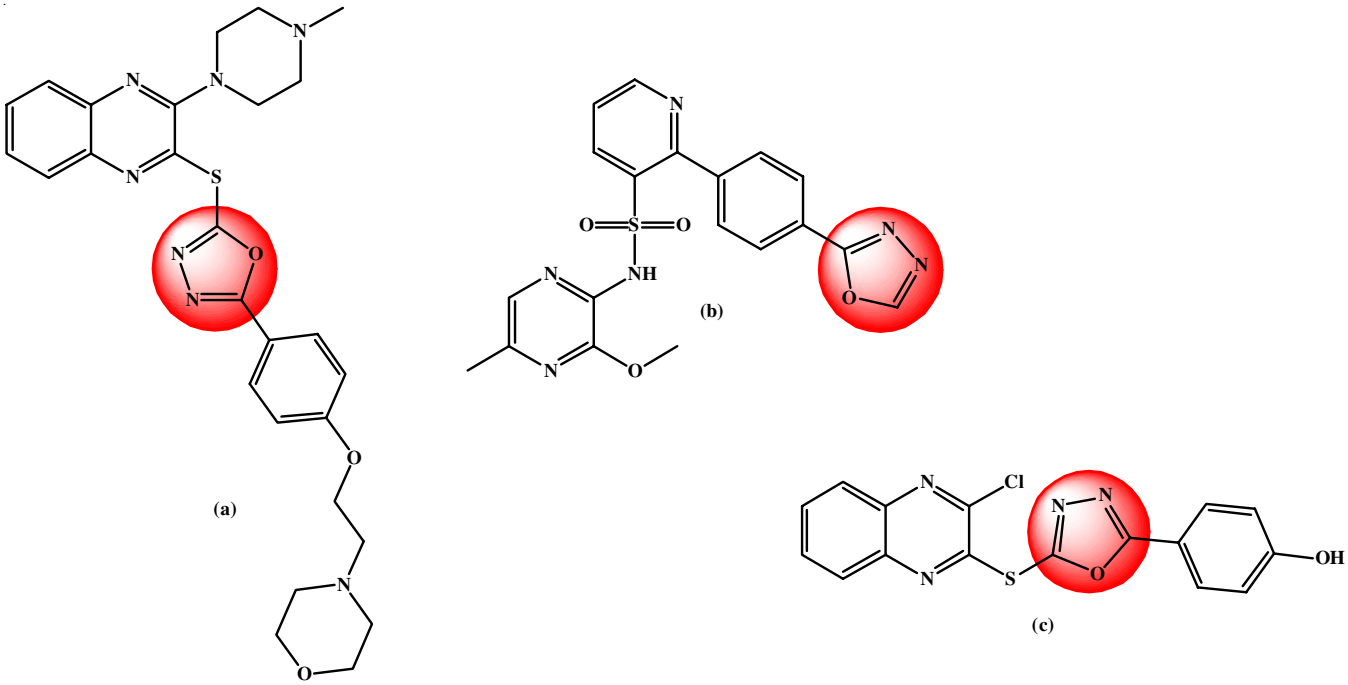


Fig. 1. Structure of the compounds having anticancer properties containing 1,3,4-oxadiazole moiety [(a) 2-[(4-morpholylethyloxy)-1,3,4-oxadiazol-2-thio]-3-N-methylpiperazilquinoxaline; (b) N-(3-methoxy-5-methyl-2-pyrazinyl)-2-[4-(1,3,4-oxadiazol-2-yl)phenyl]-3-pyridinesulfonamide; (c) 2-chloro-3-[5-(4-hydroxyphenyl)-1,3,4-oxadiazol-2-thio]quinoxaline)

## EXPERIMENTAL

**Design of 1,3,4-oxadiazole derivatives:** To design possible 1,3,4-oxadiazoles in present investigation, a thorough literature review and database searches were carried out. Prioritized were compounds with established anticancer properties (Fig. 1) and those that could be easily obtained for experimental confirmation. To achieve a thorough assessment, the selection method also took into account for 1,3,4-oxadiazole derivatives [16,17]. From the designed molecules, 20 ligands were virtually designed followed by *in silico* analysis.

### *In silico* screening

**Drug likeness and ADMET analysis:** The SwissADME server was used to assess the drug-likeness characteristics of the twenty 1,3,4-oxadiazole derivatives and pkCSM servers were used for theoretical ADMET profiling of the same [18,19].

**Synthetic accessibility study:** Synthetic accessibility study is a crucial aspect in the field of chemistry, particularly in drug discovery and development. Synthetic accessibility is the process of evaluating the simplicity and efficacy with which a compound can be synthesized or prepared in the laboratory. Synthetic accessibility study of the twenty derivatives of 1,3,4-oxadiazole were done using the SwissADME server [20].

**Protein preparation and quality assessment:** The crystal structure of BCL-2:Navitoclax (ABT-263) complex protein (Fig. 2) was selected using X-ray diffraction and retrieved from the Protein data bank (PDB ID: 4LVT, Method: X-ray diffraction, Organism: Homo sapiens, Resolution: 2.05 Å) [21-30]. The protein structure was prepared by eliminating water molecules and hetatms and modified with polar hydrogen atoms to create the proper tautomeric state [29]. The BIOVIA Discovery

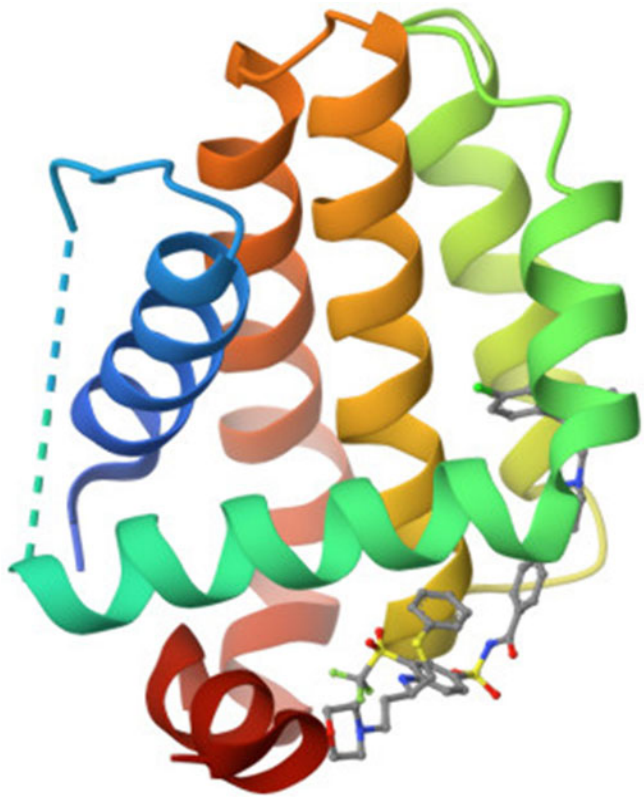

Fig. 2. 3D structure of 4LVT BCL_2-Navitoclax (ABT-263) complex

Studio was used for the preparation process and the structure was energy minimized to convert as AutoDock macromolecule [21]. Then, the prepared protein structure was energy minimized to convert as AutoDock macromolecule [15]. Quality

assessment of the protein structure was conducted using SAVES and ProSAweb server [31,32].

**Ligand preparation:** Chemical structures of all the designed 1,3,4-oxadiazoles derivatives were drawn using ACD/ ChemSketch software 12.0 and then protonated by adding hydrogen atoms with the help of BIOVIA Discovery Studio. The designed structure of 1,3,4-oxadiazoles then subjected to energy minimization with the help of the MMFF94 force field and the steepest descent algorithm [32]. The energy minimization and optimization of the compound structures were achieved with the help of Avogadro software. The optimized chemical structures further converted to AutoDock pdbqt format using OpenBabel plugin of PyRx 0.8 [26,27] and used for *in silico* analysis.

**Molecular docking:** A docking study was performed using the AutoDock Vina module of PyRx 0.8 [33,34]. In Vina Wizard, the ligand and protein structures were chosen to carry out a docking study. In the Vina workspace, a maximized grid box was selected [35]. The default value for exhaustiveness was eight [29,36]. The docked confirmation of each compound with the highest negative binding affinity was saved and 2D-3D binding interactions with targeted proteins were visualized.

***In silico* toxicity predictions:** The Protox-II online tool (https://tox-new.charite.de/protox_II/) was used to predict various toxicity end points for all compounds, including hepatotoxicity, cytotoxicity, immunogenicity, carcinogenicity and mutagenesis, demonstrating the effectiveness of computational toxicity estimations in drug design development and reducing animal experiments [37-39].

## RESULTS AND DISCUSSION

**Design of 1,3,4-oxadiazole derivatives:** 1,3,4-Oxadiazole scaffold allows for the structural modifications at different positions, leading to a diverse array of derivatives. Substituents can be introduced to tailor the compounds for specific biological targets or to enhance pharmacokinetic properties. Design of the 1,3,4-oxadiazole derivatives were done with established anticancer properties and pharmacophoric features (Table-1).

**Drug-likeness study:** The safety and drug-likeness characteristics of the twenty derivatives of 1,3,4-oxadiazoles were evaluated using the SwissADME online programme. Among the designed compounds there is violation in one parameter *i.e.* molecular weight and compounds **8** and **18** violated one criterion, according to the analysis of molecule number of hydrogen bond acceptor is greater than 10. The total polar surface area (TPSA), a crucial factor in drug bioavailability, was also calculated. Therefore, drugs that are passively absorbed and have a TPSA > 140 are regarded as having a poor oral bioavailability. Table-2 predicts that each chemical exhibits excellent log Kp values for human skin permeability and these results imply the potential use of the newly designed oxadiazole derivatives as safe lead compounds.

TABLE-1
STRUCTURE OF 1,3,4-OXADIAZOLE DERIVATIVES

| Compd. | Structure | Compd. | Structure |
|---|---|---|---|
| 1 | 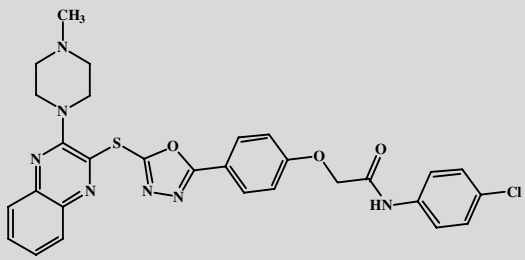 | 2 | 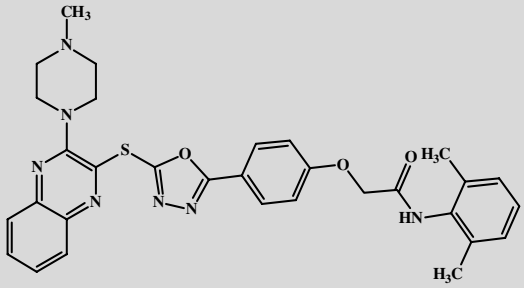 |
| 3 | 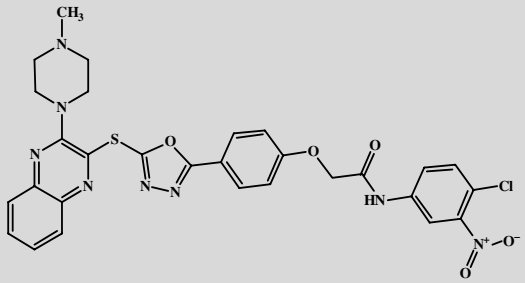 | 4 | 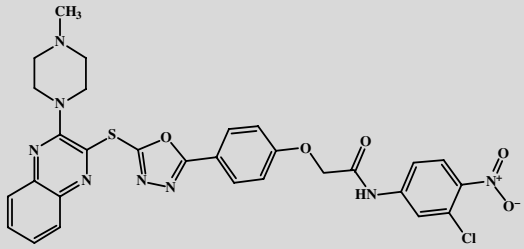 |
| 5 | 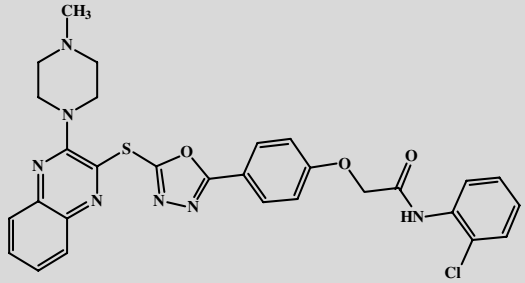 | 6 | 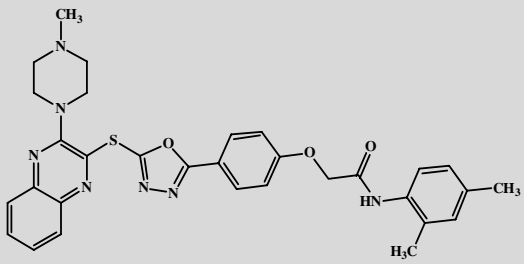 |

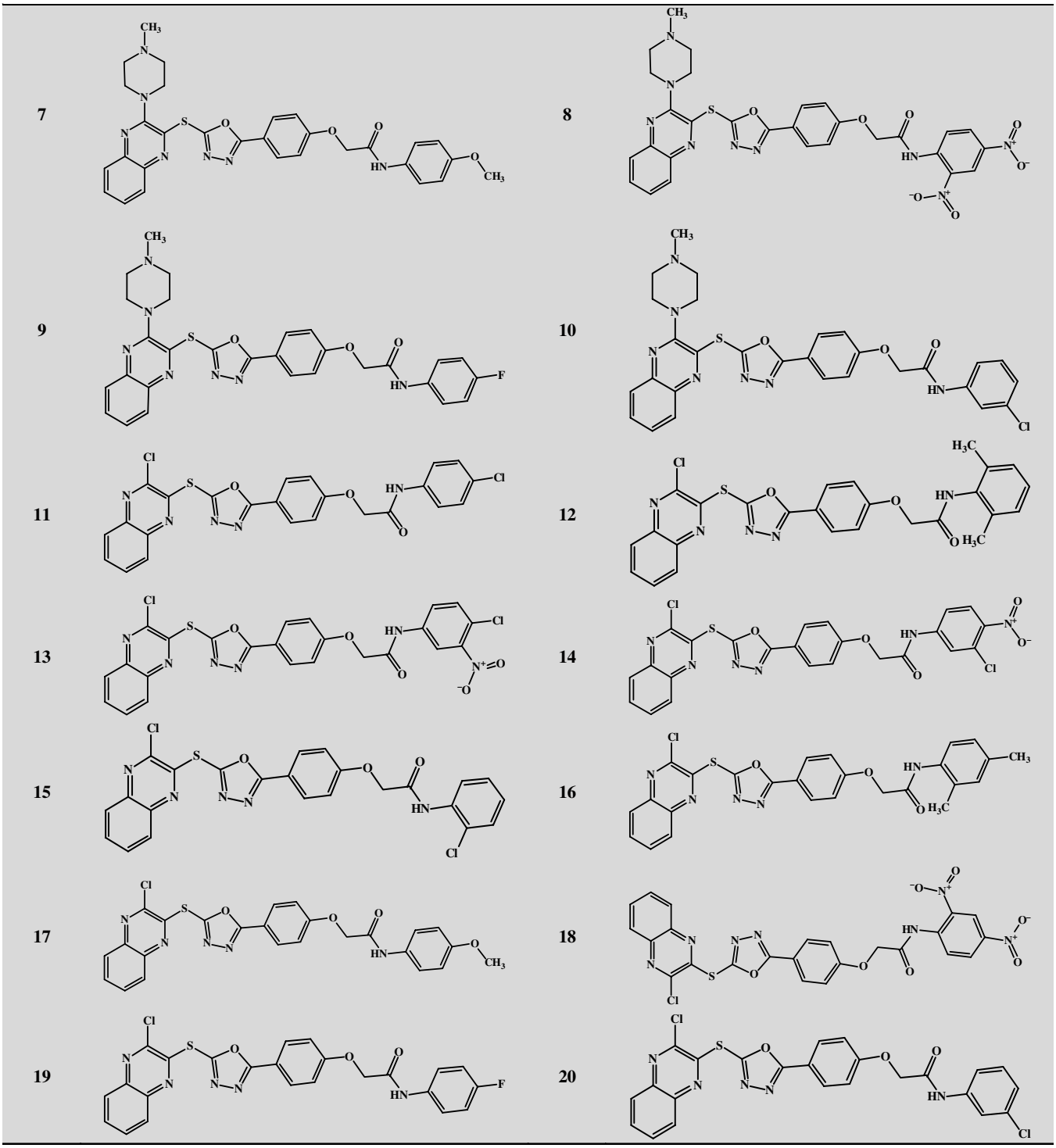

**ADMET study:** The safety and drug-likeness characteristics of 1,3,4-oxadiazoles were evaluated by the ADMET analysis (Table-3). All the compounds in present study exhibit intestinal absorption ranging from 84.77% to 100%, it suggests that these compounds have a high degree of absorption in the intestinal tract. Other results suggest that all compounds have good BBB permeability, metabolism and clearance.

**Synthetic accessibility study:** The synthetic accessibility score ranges from 1 (easy to synthesize) to 10 (hard to synthesize). Synthetic accessibility score of all twenty derivatives (Table-2) were ranges from 3.58 to 4.67, fall within a moderate to high level of synthetic accessibility. Generally, scores in this range imply that the molecules are expected to be reasonably accessible for synthesis and the procedures involved may not be overly complex. This is a favourable indication as it suggests that the compounds are likely to be viable for practical synthesis.

**Assessment of protein structure quality**

**Ramachandran plot:** The quality matrix of the protein (4LVT) was assessed using various online analytical tools. The Ramachandran plot is a crucial tool for analyzing the protein

TABLE-2
LIPINSKI's RULE OF FIVE AND DRUG-LIKENESS PREDICTION OF 1,3,4-OXADIAZOLES

| Compd. | Lipinski's rule of five | | | | | TPSA | nRot | Lipinski's Rule | Lipinski #violations | Veber Rule | Veber #violations | Synthetic accessibility |
|---|---|---|---|---|---|---|---|---|---|---|---|---|
| | MW | mLogP | nHBA | nHBD | MR | | | | | | | |
| **1** | 588.08 | 3.22 | 8 | 1 | 164.99 | 134.81 | 9 | 1 | Yes | 0 | Yes | 4.33 |
| **2** | 581.69 | 3.14 | 8 | 1 | 169.91 | 134.81 | 9 | 1 | Yes | 0 | Yes | 4.61 |
| **3** | 633.08 | 2.44 | 10 | 1 | 173.81 | 180.63 | 10 | 2 | No | 1 | No | 4.50 |
| **4** | 633.08 | 2.44 | 10 | 1 | 173.81 | 180.63 | 10 | 2 | No | 1 | No | 4.44 |
| **5** | 588.08 | 3.22 | 8 | 1 | 164.99 | 134.81 | 9 | 1 | Yes | 0 | Yes | 4.35 |
| **6** | 581.69 | 3.14 | 8 | 1 | 169.91 | 134.81 | 9 | 1 | Yes | 0 | Yes | 4.60 |
| **7** | 583.66 | 2.45 | 9 | 1 | 166.47 | 144.04 | 10 | 2 | No | 1 | No | 4.51 |
| **8** | 643.63 | 1.25 | 12 | 1 | 177.62 | 226.45 | 11 | 2 | No | 2 | No | 4.67 |
| **9** | 571.63 | 3.12 | 9 | 1 | 159.94 | 134.81 | 9 | 1 | Yes | 0 | Yes | 4.35 |
| **10** | 588.08 | 3.22 | 8 | 1 | 164.99 | 134.81 | 9 | 1 | Yes | 0 | Yes | 4.34 |
| **11** | 524.38 | 3.57 | 7 | 1 | 133.74 | 128.33 | 8 | 1 | Yes | 0 | Yes | 3.58 |
| **12** | 517.99 | 3.5 | 7 | 1 | 138.66 | 128.33 | 8 | 1 | Yes | 0 | Yes | 3.83 |
| **13** | 569.38 | 3.29 | 9 | 1 | 142.56 | 174.15 | 9 | 2 | No | 1 | No | 3.77 |
| **14** | 569.38 | 3.29 | 9 | 1 | 142.56 | 174.15 | 9 | 2 | No | 1 | No | 3.68 |
| **15** | 524.38 | 3.57 | 7 | 1 | 133.74 | 128.33 | 8 | 1 | Yes | 0 | Yes | 3.60 |
| **16** | 517.99 | 3.5 | 7 | 1 | 138.66 | 128.33 | 8 | 1 | Yes | 0 | Yes | 3.82 |
| **17** | 519.96 | 2.79 | 8 | 1 | 135.22 | 137.56 | 9 | 1 | Yes | 0 | Yes | 3.74 |
| **18** | 579.93 | 2.06 | 11 | 1 | 146.37 | 219.97 | 10 | 2 | No | 1 | No | 3.93 |
| **19** | 507.92 | 3.47 | 8 | 1 | 128.69 | 128.33 | 8 | 1 | Yes | 0 | Yes | 3.58 |
| **20** | 524.38 | 3.57 | 7 | 1 | 133.74 | 128.33 | 8 | 1 | Yes | 0 | Yes | 3.58 |

TABLE-3
PREDICTED *in silico* ADMET PROPERTIES FOR 1,3,4-OXADIAZOLES

| Compd. | Absorption | Distribution | | | Metabolism | | | | | | | Excretion | Toxicity |
|---|---|---|---|---|---|---|---|---|---|---|---|---|---|
| | Intestinal absorption (human) | VDSs (human) | BBB permeability | CNS permeability | Substrate | | Inhibitors | | | | | Total clearance | AMES toxicity |
| | | | | | CYP | | | | | | | | |
| | | | | | 2D6 | 3A4 | 1A2 | 2C19 | 2C9 | 2D6 | 3A4 | | |
| | Numeric (% absorbed) | Numeric (log L $kg^{-1}$) | Numeric (log BB) | Numeric (log PS) | Categorical (Yes/No) | | | | | | | Numeric (log mL $min^{-1}$ $kg^{-1}$) | Categorical (Yes/No) |
| **1** | 92 | 0.123 | -1.298 | -3.288 | No | Yes | No | Yes | Yes | No | Yes | 0.264 | No |
| **2** | 91.81 | 0.181 | -1.119 | -3.243 | No | Yes | No | No | Yes | No | Yes | 0.24 | No |
| **3** | 89 | -0.374 | -1.674 | -3.387 | No | Yes | No | Yes | Yes | No | Yes | -0.068 | No |
| **4** | 88.96 | -0.316 | -1.705 | -3.41 | No | Yes | No | Yes | Yes | No | Yes | -0.113 | No |
| **5** | 92 | 0.123 | -1.298 | -3.288 | No | Yes | No | Yes | Yes | No | Yes | 0.286 | No |
| **6** | 91.8 | 0.153 | -1.099 | -3.252 | No | Yes | No | No | Yes | No | Yes | 0.239 | No |
| **7** | 90.42 | 0.099 | -1.737 | -3.646 | No | Yes | No | No | Yes | No | Yes | 0.402 | No |
| **8** | 84.77 | -0.861 | -1.942 | -3.585 | No | Yes | No | Yes | Yes | No | Yes | -0.266 | No |
| **9** | 88.98 | 0.025 | -1.33 | -3.407 | No | Yes | No | No | Yes | No | Yes | 0.288 | No |
| **10** | 92.04 | 0.123 | -1.288 | -3.288 | No | Yes | No | Yes | Yes | No | Yes | 0.198 | No |
| **11** | 100 | 0.381 | -1.27 | -3.049 | No | Yes | No | Yes | Yes | No | Yes | -0.287 | No |
| **12** | 100 | 0.444 | -1.089 | -3.014 | No | Yes | No | Yes | Yes | No | Yes | -25 | No |
| **13** | 98.61 | 0.02 | -1.656 | -3.217 | No | Yes | No | Yes | Yes | No | Yes | -0.139 | No |
| **14** | 98.61 | 0.057 | -1.653 | -3.217 | No | Yes | No | Yes | Yes | No | Yes | -0.141 | No |
| **15** | 100 | 0.381 | -1.27 | -3.049 | No | Yes | No | Yes | Yes | No | Yes | -0.019 | No |
| **16** | 100 | 0.416 | -1.071 | -3012 | No | Yes | No | Yes | Yes | No | Yes | -0.254 | No |
| **17** | 97.61 | -0.093 | -1.608 | -3.429 | No | Yes | No | Yes | Yes | No | Yes | -0.128 | No |
| **18** | 94.25 | -0.413 | -1.899 | -3.47 | No | Yes | No | Yes | Yes | No | Yes | 0.038 | No |
| **19** | 98.89 | 0.256 | -1.303 | -3.234 | No | Yes | No | Yes | Yes | No | Yes | -0.307 | No |
| **20** | 100 | 0.381 | -1.27 | -3.049 | No | Yes | No | Yes | Yes | No | Yes | -0.226 | No |

secondary structure, predicting that a high-quality protein should have over 90% amino acid residues in its most favourable regions [40-43]. As per result (Fig. 3a), 95.5% of the residues are in the most favoured regions.

**ERRAT study:** The ERRAT score measures non-bonded interactions between atoms and plots the error function against a sliding window. It indicates the confidence in rejecting regions exceeding the error value. The overall quality factor is expressed as the percentage of proteins below the 95% rejection limit [39]. According to the results (Fig. 3b), ERRAT score was found to be 96.17% which is higher than 95% showed that the protein structure is having good high quality resolution structure.

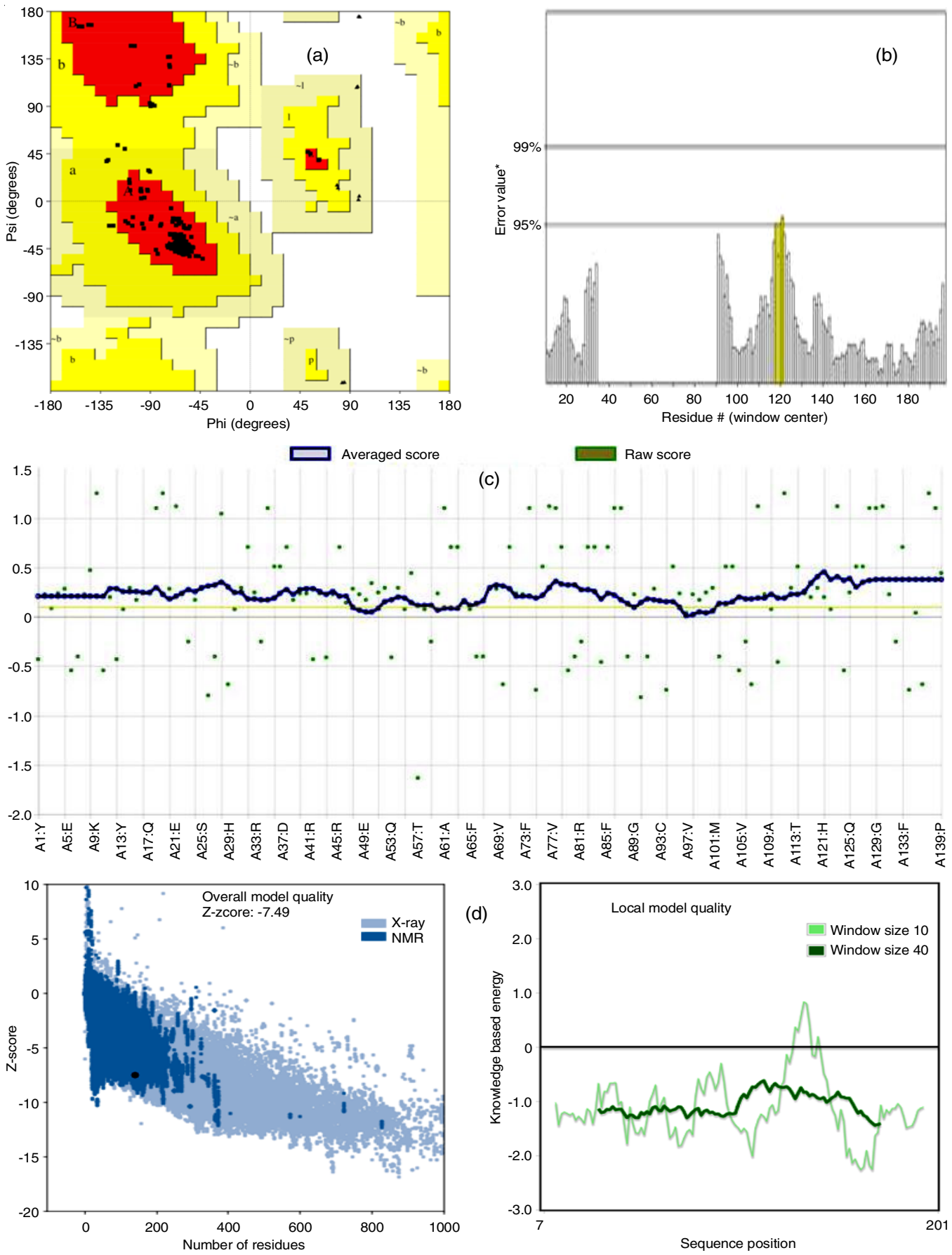


Fig. 3. (a) Ramachandran plot, (b) ERRAT chart, (c) VERIFY3D chart and (d) ProSA chart

**Verify3D analysis:** The Verify3D score assesses the compatibility of an atomic model (3D) with its amino acid sequence (1D), ensuring at least 80% of amino acid residues score above 0.1 [31,44]. As per the resulted Verify3D score (Fig. 3c) 90.65% of the amino acid residues scored >= 0.1.

**ProSA-web study:** ProSA-web is a program used in the protein structure validation to identify errors in experimental and theoretical protein models. It calculates an overall quality score for a specific input structure, which indicates model quality. The z-score, displayed in a plot, helps check if the input structure's score is within the range of native proteins. As per the results, Z-score is found to be -7.49.

**Plot of residue scores:** The plot of residue scores displays the quality of the local model by plotting energies in relation to amino acid sequence position i. Positive values indicate incorrect or problematic elements in the input structure. Since single residue energies fluctuate a lot, they are not ideal for evaluating models [45]. To smooth the chart, the average energy of each 40-residue fragment is calculated and assigned to the 'central' residue at position i+19. In the background, there is a second line that has a window size of only 10 residues. All of the results validated the 3D structure's exceptional quality and dependability, making it a great choice for more *in silico* studies.

**Molecular docking study:** To get further insight into the efficacy of the developed compounds, the interactions between the oxadiazole derivatives and the protein crystal structure were examined. The BCL-2 protein (PDB ID: 4LVT) was our choice to interact with the target compounds [46]. The predicted docking score (kcal/mol) was used as the ranking criterion. Target compounds 1 to 20 and their docking interaction results with the target protein are listed in Table-4 & Fig. 4. Docking scores for compounds **1** to **20** ranged from -9.9 to -11.2 kcal/mol. With docking scores of -11.2 and -10.9, respectively, the two most powerful compounds in this series are 2 and 5. The results showed that compound **2** had a π-alkyl interaction with ALA97, MET112, VAL153, PHE109, ALA146, VAL145 and ASN140 protein residues by a hydrogen bond. It also exhibit π-π interactions with PHE101 and TYR105. Compound **5** made two CH bonds with the protein residues ARG104 and ASP108. Additionally, it created two π-π interactions with PHE101 and TYR105, as well as π-alkyl links with MET112, VAL145, ALA97, ALA146, ARG143 and LEU134. The ability of the target molecule to engage with significant amino acids in the

TABLE-4
DOCKING INTERACTION RESULTS OF 1,3,4-OXADIAZOLES WITH TARGET PROTEIN

| Compd. | Binding affinity (kcal/mol) | Interacting residues | Type of interactions |
|---|---|---|---|
| **1** | -10.5 | GLY142, GLU111, ASP108<br>TYR105, PHE101<br>MET112, ALA97, PHE195, LEU198, TYR199, VAL145, ARG143, ALA146 | CH Bond<br>Pi-Pi T-Shaped<br>Alkyl, Pi-Alkyl |
| **2** | -11.2 | ASN140<br>PHE101, TYR105<br>ARG143, MET112, VAL153, PHE109, ALA146, VAL145, ALA97 | H Bond<br>Pi-Pi T-Shaped<br>Alkyl, Pi-Alkyl |
| **3** | -10.2 | ASP108<br>LEU134 MET112<br>PHE101<br>ALA97, TYR199, ALA146, ARG143, MET112 | CH Bond<br>Pi-Sigma<br>Pi-Pi T-Shaped<br>Alkyl, Pi-Alkyl |
| **4** | -10.1 | ASP108, GLU111<br>MET112<br>TYR105, PHE101<br>ARG143, LEU198, ALA146, LEU134, MET112 | CH Bond<br>Pi-Sigma<br>Pi-Pi T-Shaped<br>Alkyl, Pi-Alkyl |
| **5** | -10.9 | ARG104, ASP108<br>MET112<br>TYR105, PHE101<br>ALA146, VAL145, ALA97, ARG143, LEU134, MET112 | CH Bond<br>Pi-Sigma<br>Pi-Pi T-Shaped<br>Alkyl, Pi-Alkyl |
| **6** | -10.8 | ASP108, GLU111<br>PHE101, TYR105<br>LEU134, ARG143, ALA97, PHE195, LEU198, TYR199, VAL145, ALA146, MET112 | CH Bond<br>Pi-Pi T-Shaped<br>Alkyl, Pi-Alkyl |
| **7** | -9.9 | ASP108, GLU111, TYR199<br>MET112<br>PHE101, TYR105<br>LEU134, MET112, TYR199, ARG143, ALA146 | CH Bond<br>Pi-Sigma<br>Pi-Pi T-Shaped<br>Alkyl, Pi-Alkyl |
| **8** | -10.4 | ASP108<br>MET112<br>PHE101, TYR105<br>ARG143, LEU134, MET112, ALA146 | CH Bond<br>Pi-Sigma<br>Pi-Pi T-Shaped<br>Alkyl, Pi-Alkyl |
| **9** | -10.6 | ASP108<br>ALA97<br>LEU134, MET112<br>ASP100<br>ALA97, VAL145, ARG143, ALA146, MET112 | CH Bond<br>Halogen (Fluorine)<br>Pi-Sigma<br>Amide-Pi Stacked<br>Alkyl, Pi-Alkyl |

| | | | |
|---|---|---|---|
| **10** | -10.8 | ASP108 | CH Bond |
| | | MET112 | Pi-Sigma |
| | | PHE101, TYR105 | Pi-Pi T-Shaped |
| | | LEU134, ALA146, ALA97, PHE195, TYR199, ARG143, VAL145, MET112 | Alkyl, Pi-Alkyl |
| **11** | -10.4 | ALA97 | Halogen (Cl, Br, I) |
| | | TYR105 | Pi-Sulfur |
| | | PHE101, TYR105 | Pi-Pi T-Shaped |
| | | ALA97, ALA146, PHE109, VAL153, MET112, LEU1980 | Alkyl, Pi-Alkyl |
| **12** | -10.4 | MET112 | Pi-Sigma |
| | | LEU134, ARG143, ALA97, VAL145, ALA146, MET112 | Alkyl, Pi-Alkyl |
| **13** | -10 | LEU134, MET112 | Pi-Sigma |
| | | ARG143, ALA97, TYR199, ALA146, MET112 | Alkyl, Pi-Alkyl |
| **14** | -10.5 | TYR199 | CH Bond |
| | | ASP108 | Pi-Anion |
| | | MET112 | Pi-Sigma |
| | | PHE101, TYR105 | Pi-Pi T-Shaped |
| | | ARG143, ALA146, MET112 | Alkyl, Pi-Alkyl |
| **15** | -10.7 | TYR105 | Pi-Sulfur |
| | | PHE101, GLY142 | Pi-Pi T-Shaped |
| | | TYR105 | Amide-Pi Stacked |
| | | ALA97, VAL145, ARG143, MET112, ALA146, LEU198 | Pi-Alkyl |
| **16** | -10.8 | TYR105, PHE101 | Pi-Pi T-Shaped |
| | | ARG143, LEU134, MET112, ALA146, PHE195, ALA97, LEU198 | Alkyl, Pi-Alkyl |
| **17** | -9.9 | GLY142 | CH Bond |
| | | TYR105, PHE101 | Pi-Sulfur |
| | | TYR105, PHE101 | Pi-Pi Stacked |
| | | TYR105, PHE101 | Pi-Pi T-Shaped |
| | | VAL145, LEU198, PHE109, VAL153, MET112, ALA146 | Alkyl, Pi-Alkyl |
| **18** | -10.1 | PHE109, PHE150, GLY142 | CH Bond |
| | | ALA97 | Halogen (Cl, Br, I) |
| | | TYR105, PHE101 | Pi-Sulfur |
| | | TYR105, PHE101 | Pi-Pi Stacked |
| | | PHE195, PHE101 | Pi-Pi T-Shaped |
| | | ALA97, LEU198, ARG143, MET112, ALA146 | Alkyl, Pi-Alkyl |
| **19** | -10.7 | PHE150 | CH Bond |
| | | TYR105 | Pi-Sulfur |
| | | PHE101, TYR105 | Pi-Pi T-Shaped |
| | | GLY142 | Amide-Pi Stacked |
| | | ALA146, ARG143, PHE101, VAL145, ALA97, LEU198, MET112 | Alkyl, Pi-Alkyl |
| **20** | -10.4 | MET112 | Pi-Sigma |
| | | PHE101, TYR105 | Pi-Pi T-Shaped |
| | | ALA146, MET112, ALA97, VAL145, TYR199, PHE195, ARG143 | Alkyl, Pi-Alkyl |

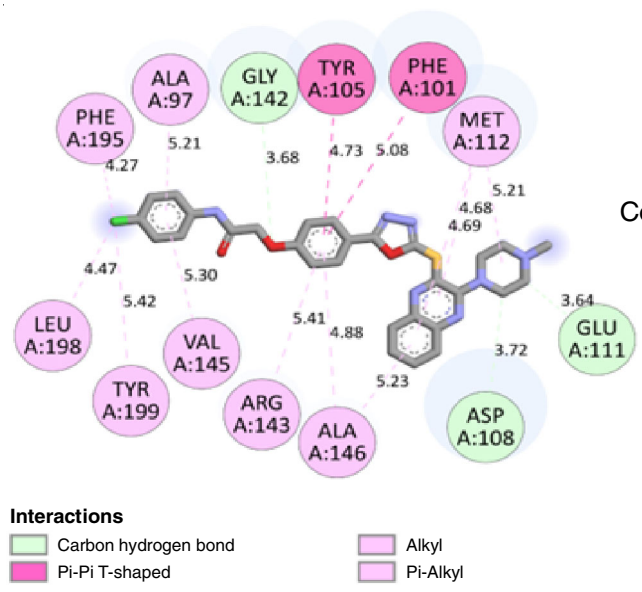


Compd. **1**

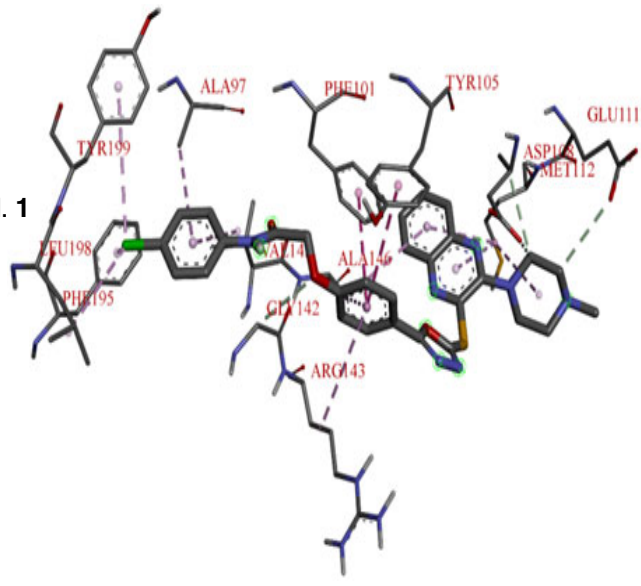

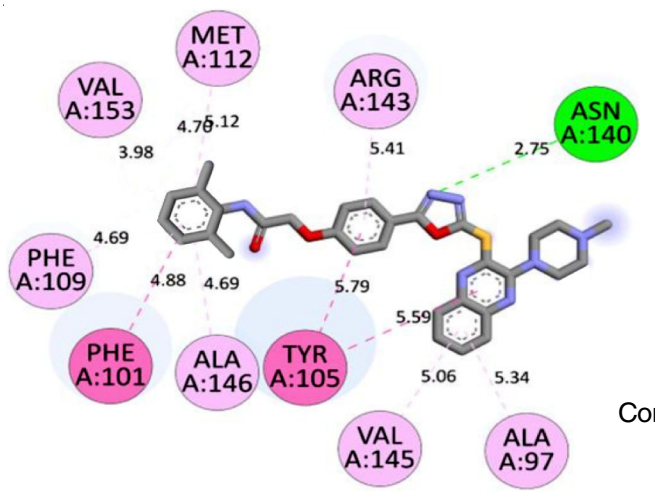


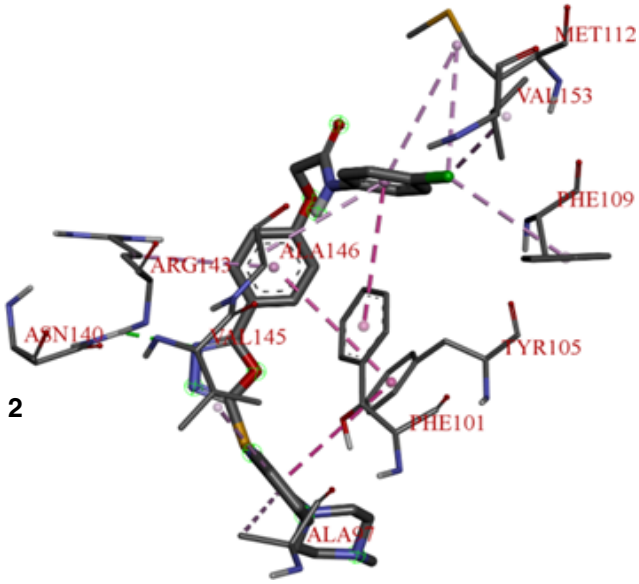


**Interactions**

Carbon hydrogen bond
Pi-Pi T-shaped
Alkyl
Pi-Alkyl

Compd. **2**

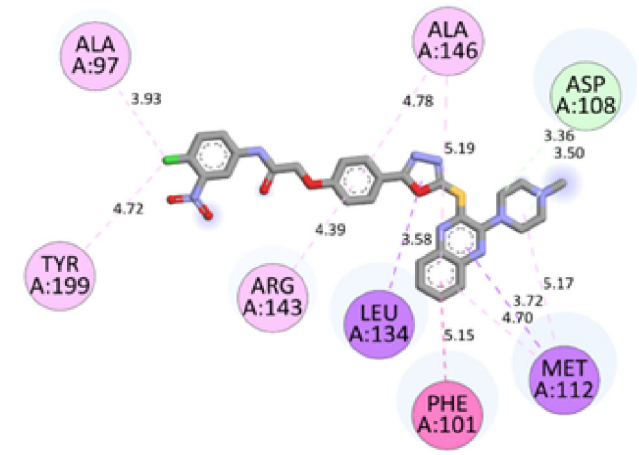


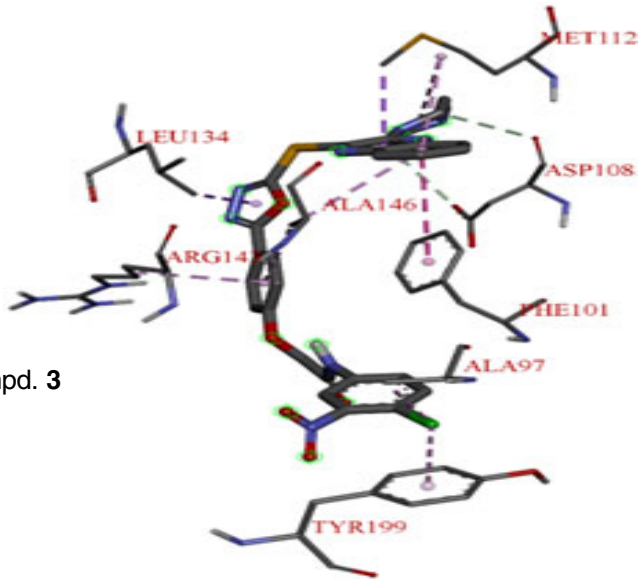


**Interactions**

Carbon hydrogen bond
Pi-Sigma
Pi-Pi T-shaped
Alkyl
Pi-Alkyl

Compd. **3**

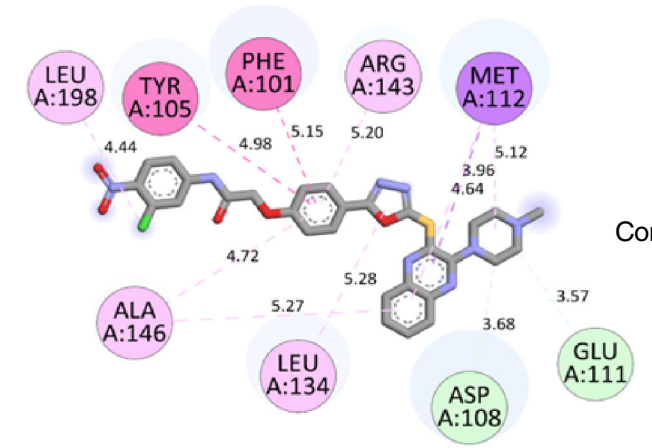


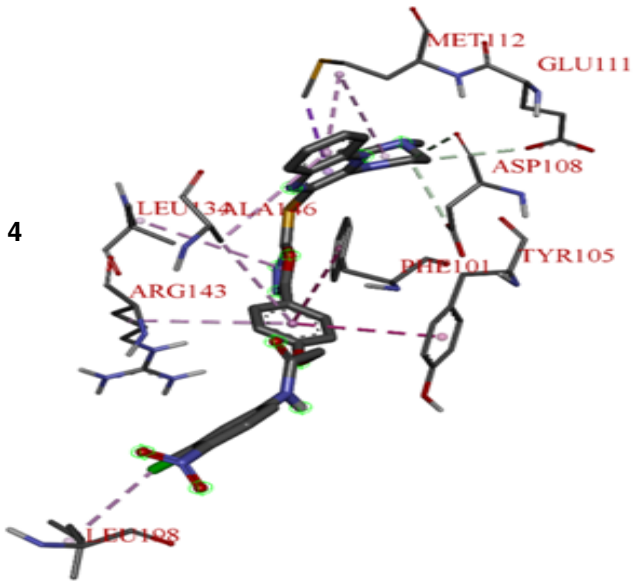


**Interactions**

Carbon hydrogen bond
Pi-Sigma
Pi-Pi T-shaped
Alkyl
Pi-Alkyl

Compd. **4**

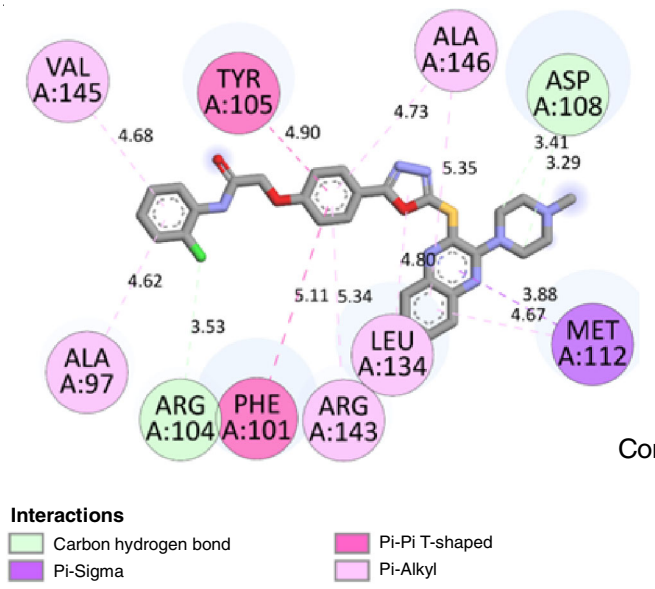


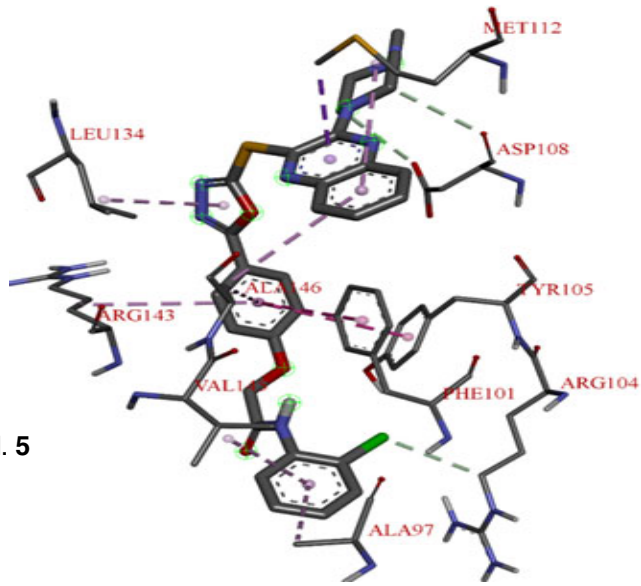


Compd. **5**

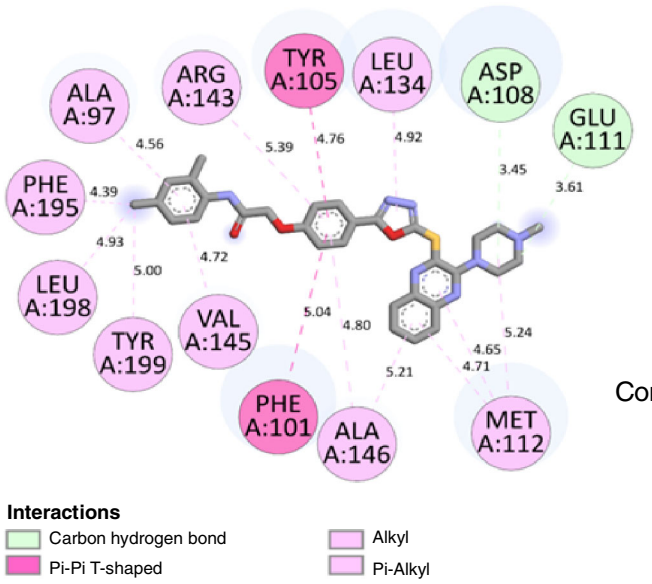


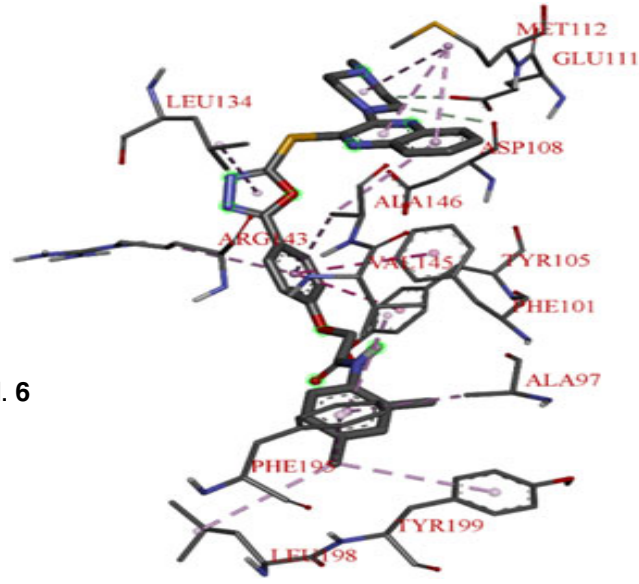


Compd. **6**

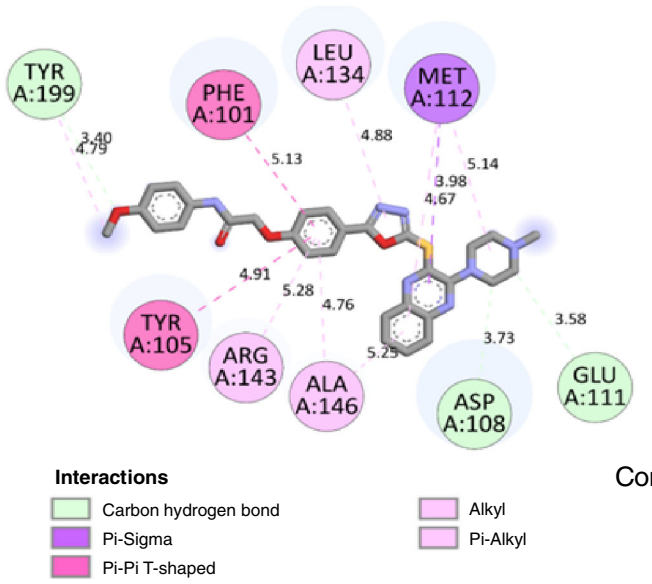


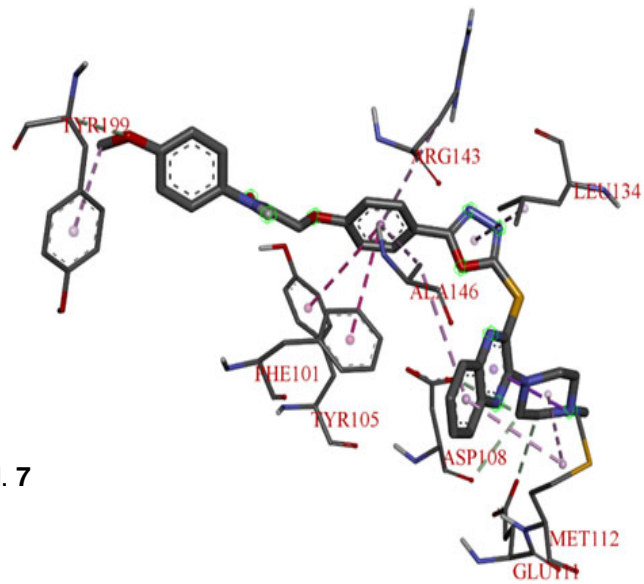


Compd. **7**

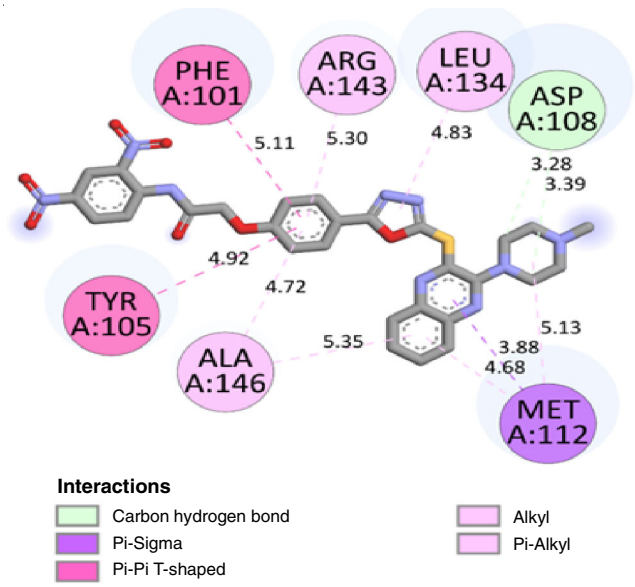


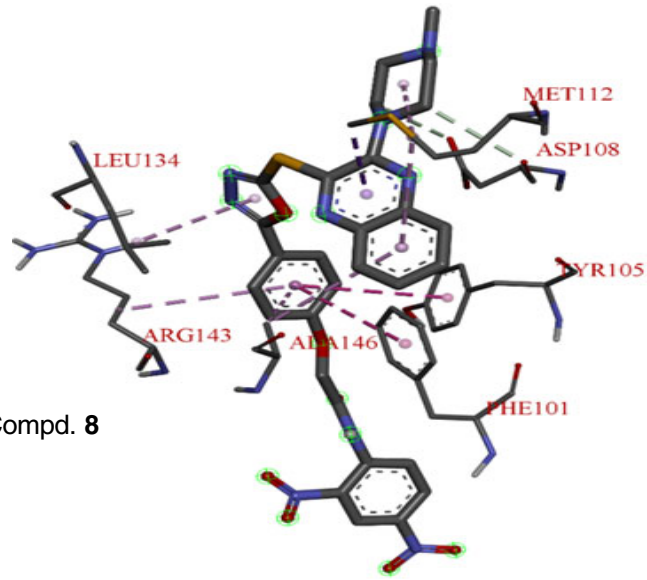


Compd. **8**

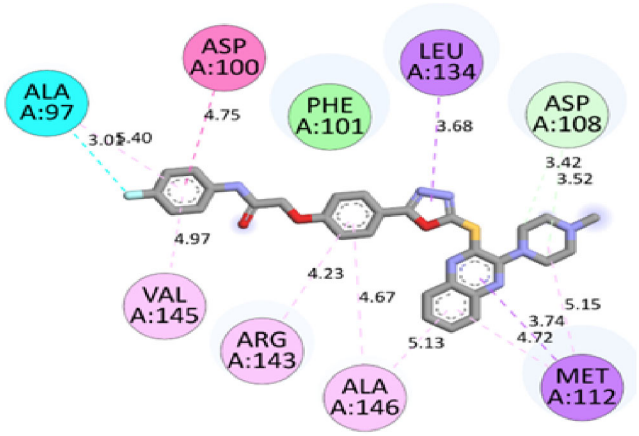


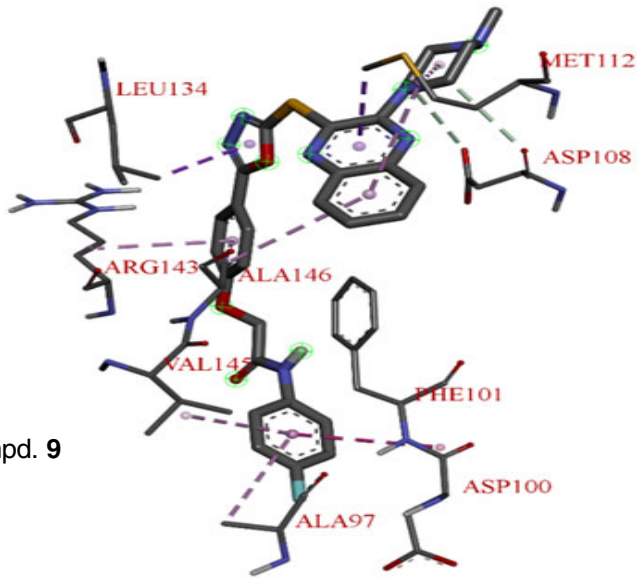


Compd. **9**

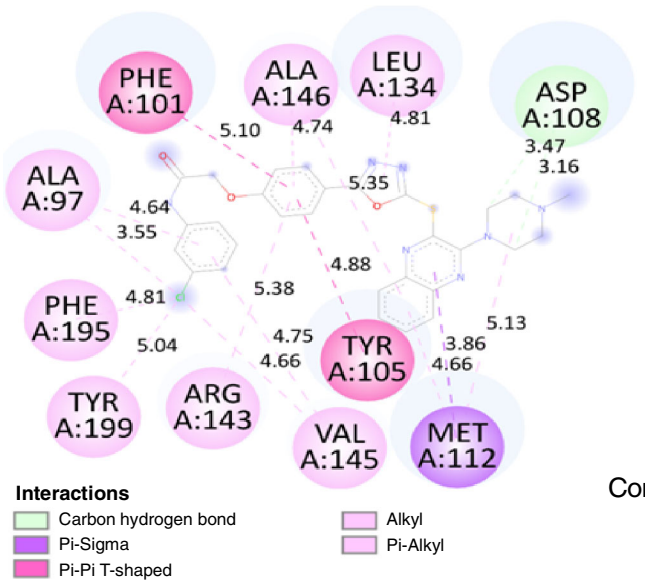


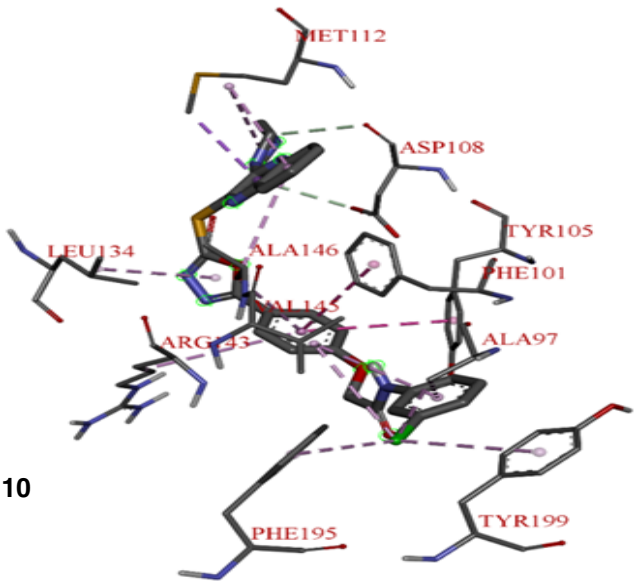


Compd. **10**

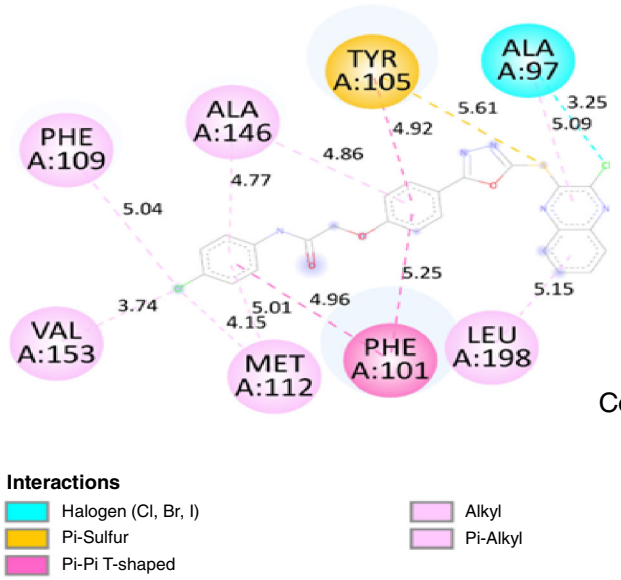


Compd. **11**

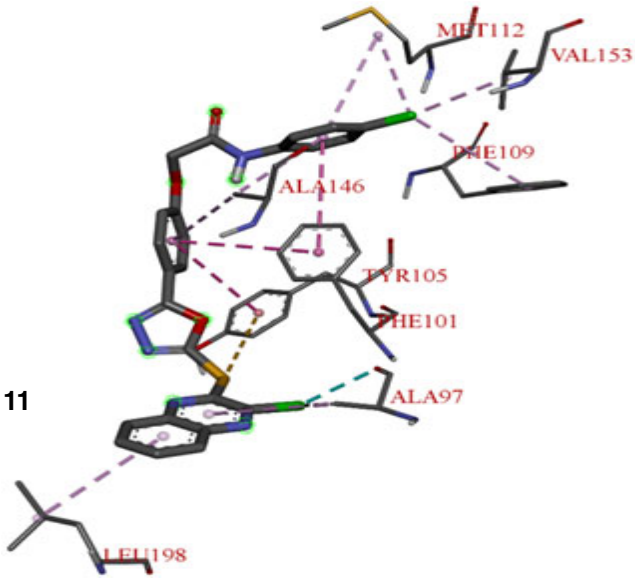


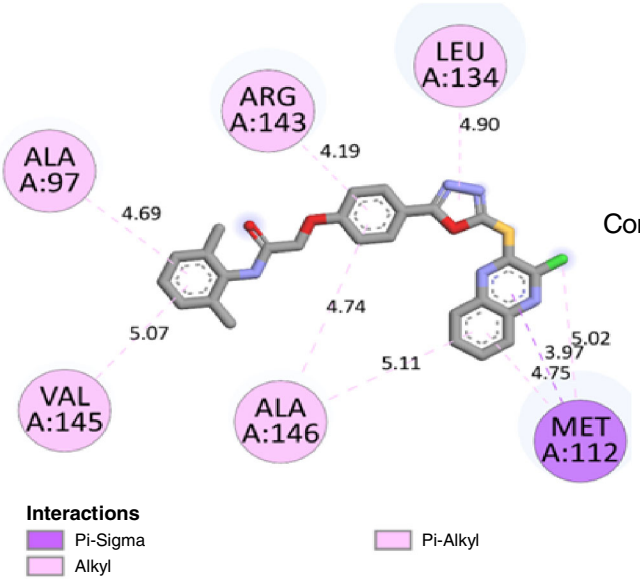


Compd. **12**

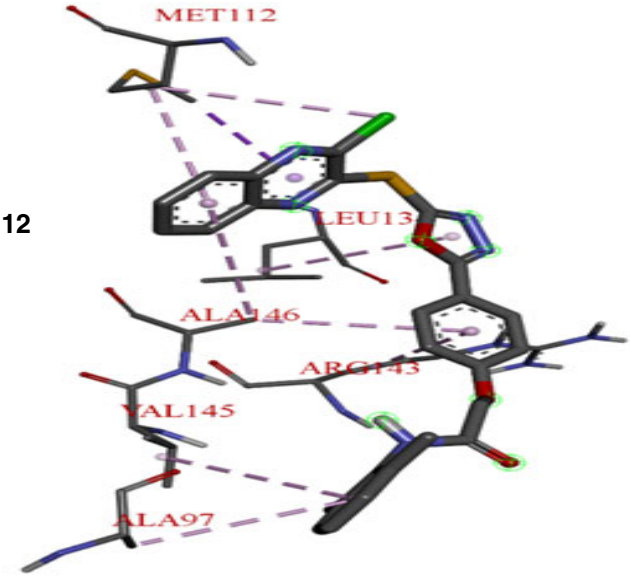


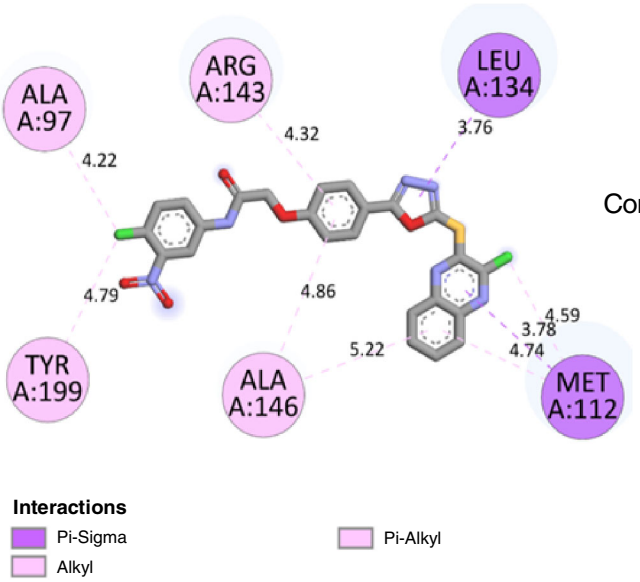


Compd. **13**

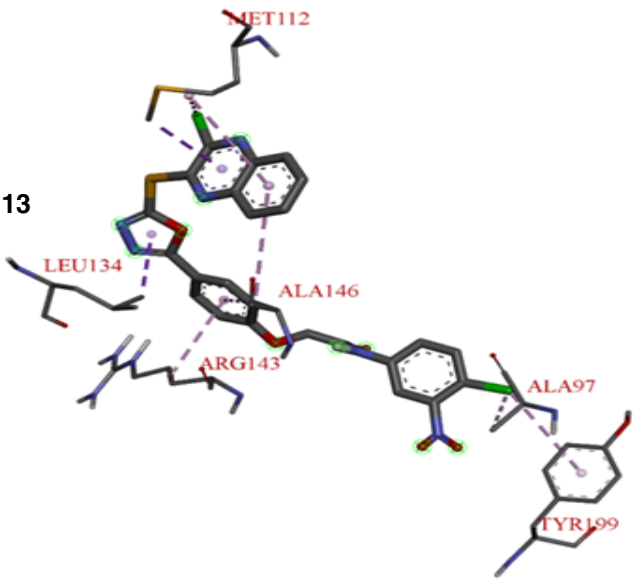

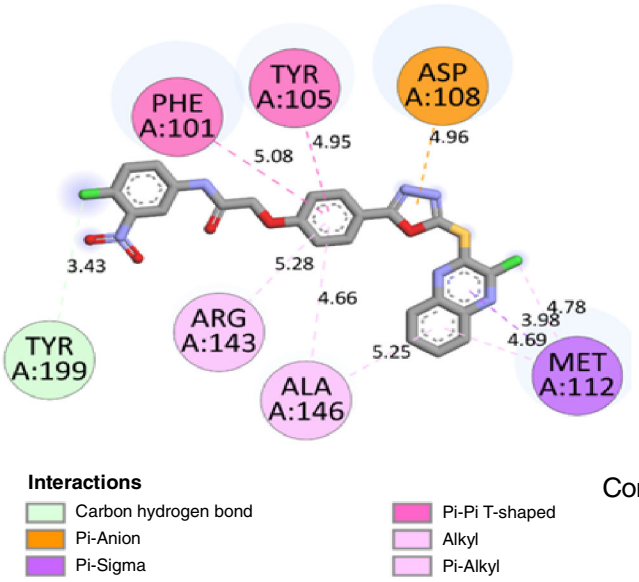


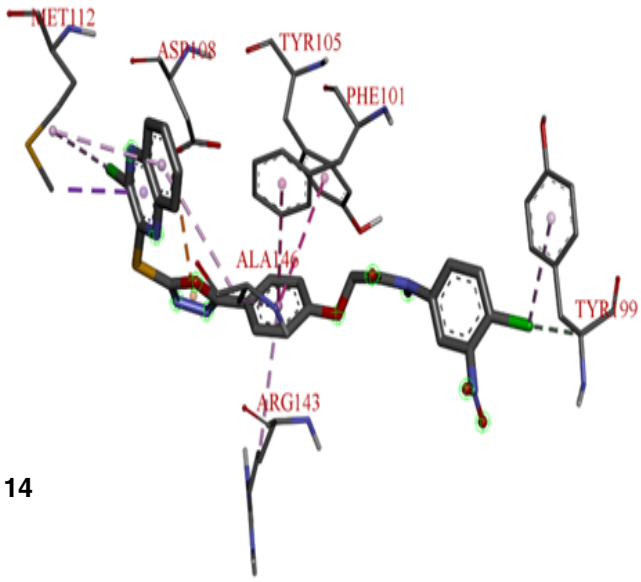


Compd. **14**

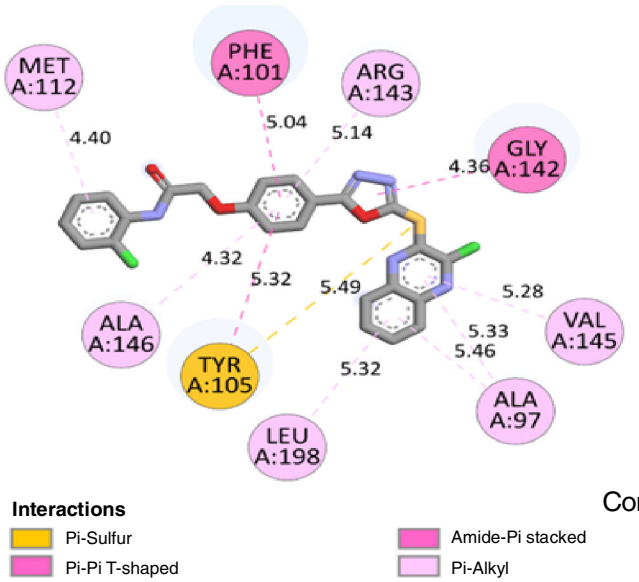


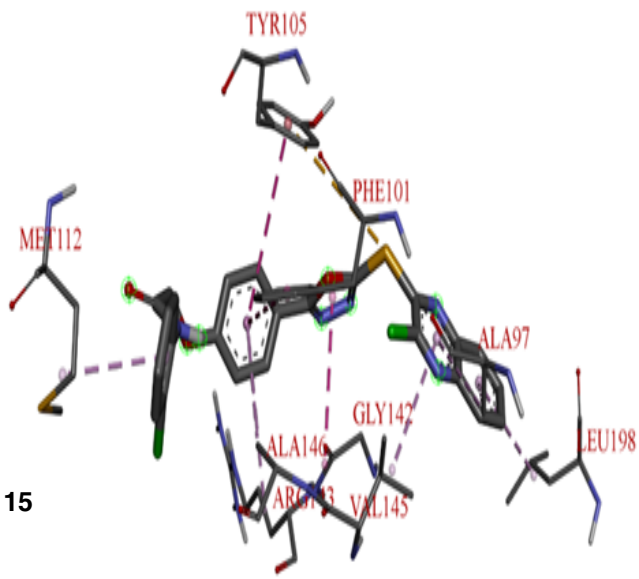


Compd. **15**

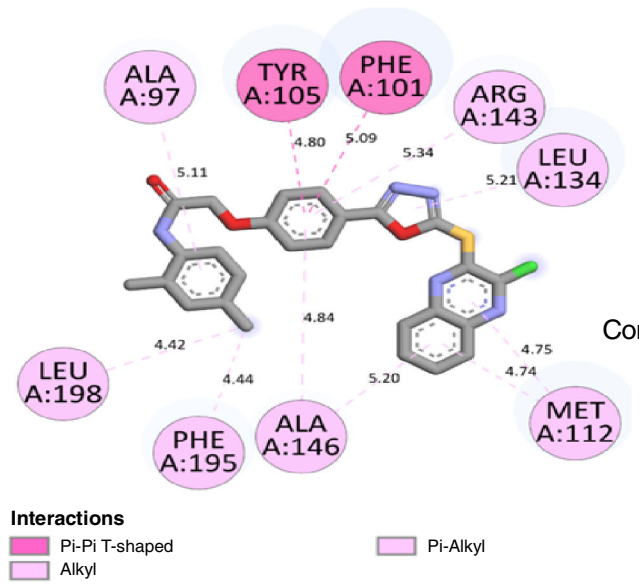


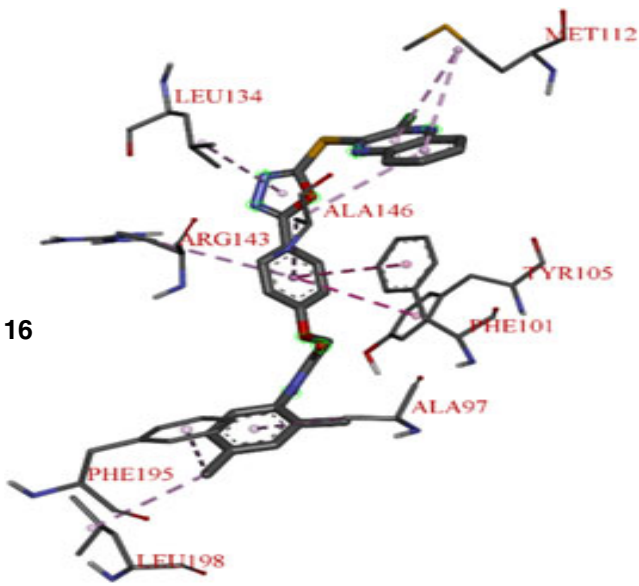


Compd. **16**

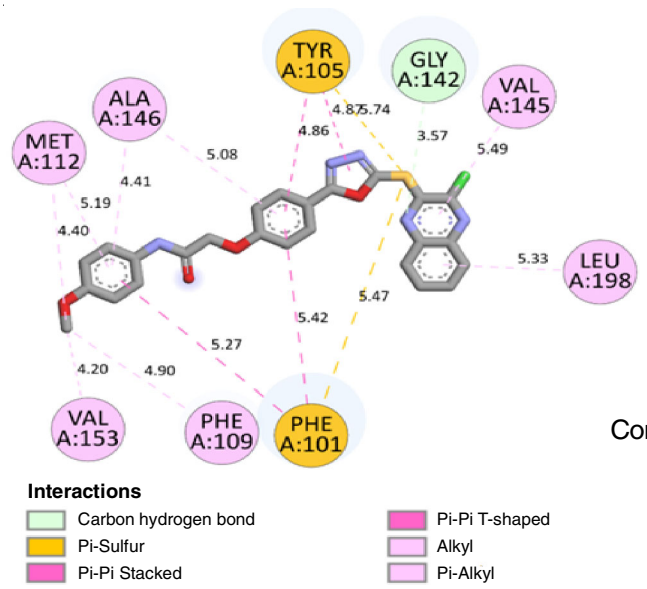


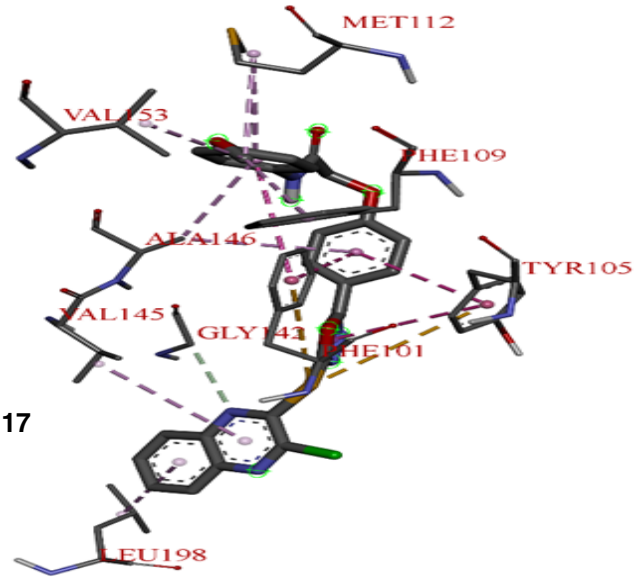


Compd. **17**

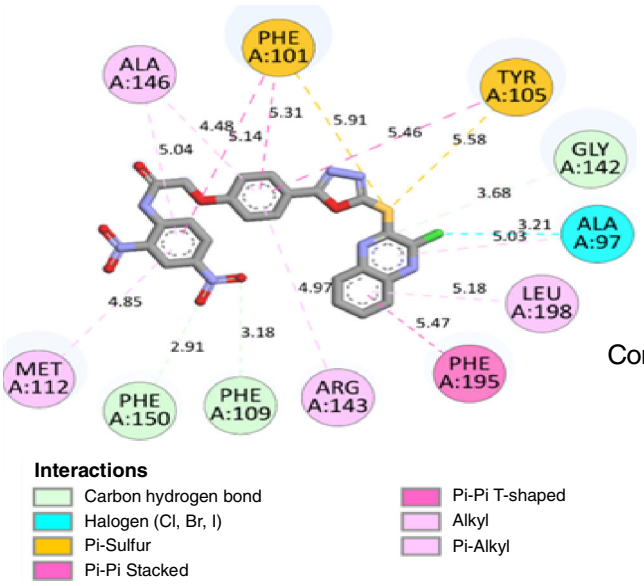


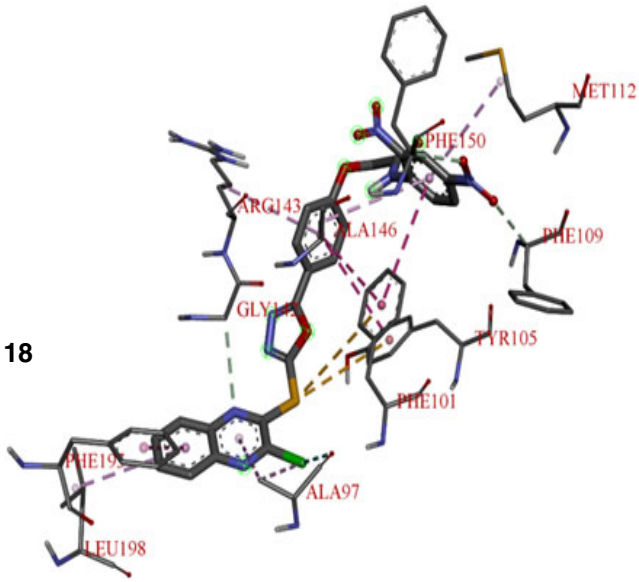


Compd. **18**

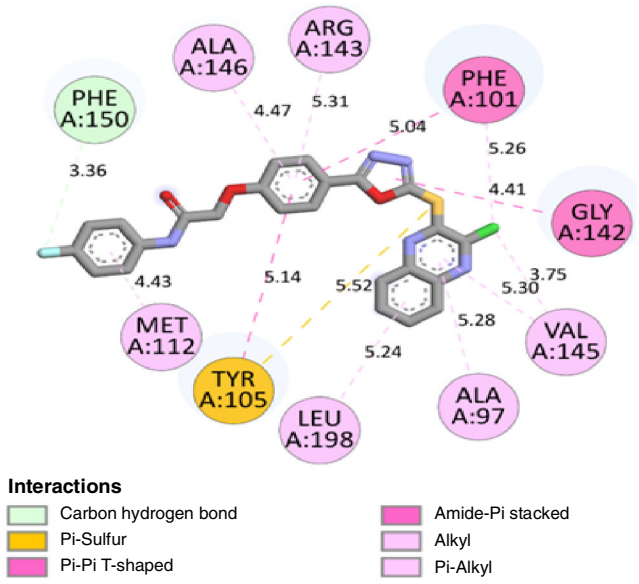


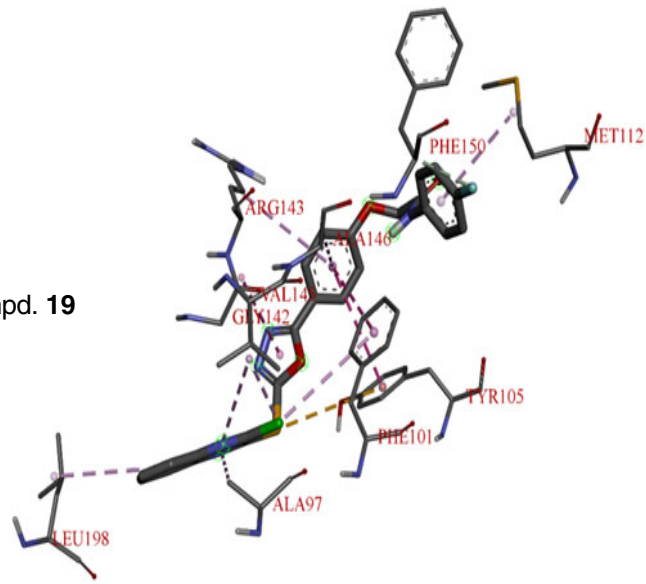


Compd. **19**

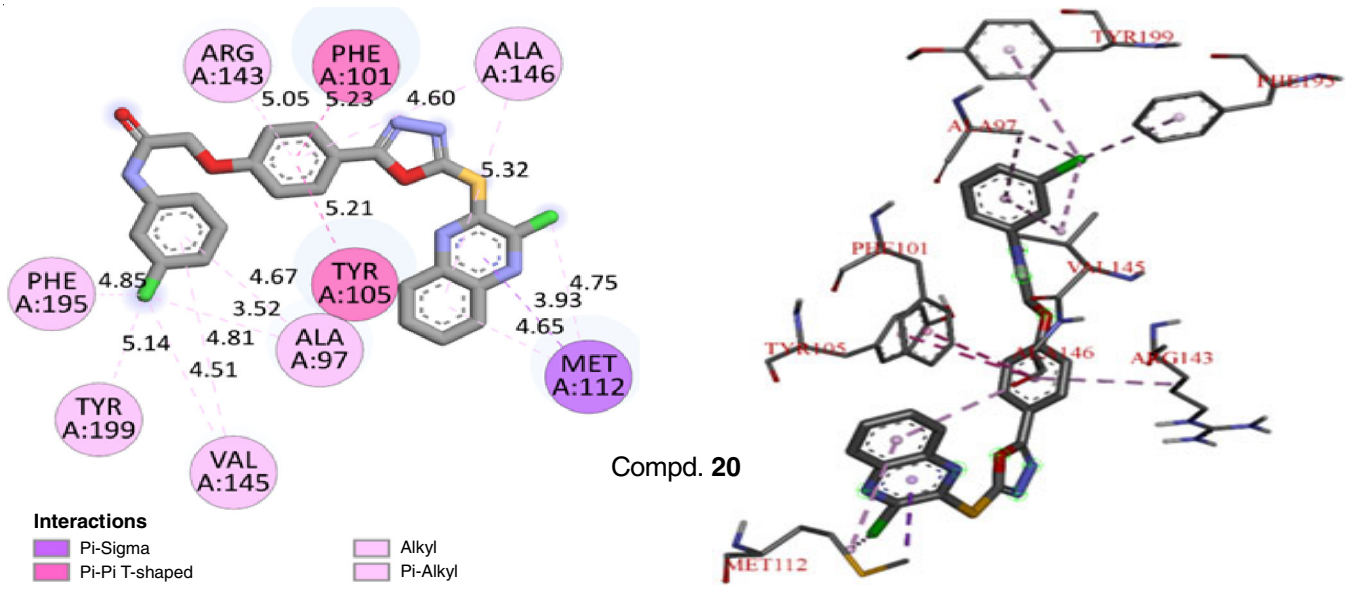


Fig. 4. 2D and 3D binding interaction between compounds **1-20** and targeted protein

target protein binding region supports its strong action, as shown by its high docking score and pattern [47]. The results of the molecular docking investigations agreed compounds **2** and **5** shown a notable cytotoxic.

***In silico* toxicity predictions:** The prediction of organ toxicity (hepatotoxicity) as well as various toxicity end points like cytotoxicity, immunogenicity, carcinogenicity, mutagenesis were computed for all compounds (Table-5). Every compound displayed an active hepatotoxicity profile, with the exception of compounds **2** and **6**. Compounds **11**, **12**, **15**, **16**, **17**, **19** and **20** exhibited no activity for the immunotoxicity, mutagenicity, cytotoxicity and carcinogenicity, hence these compounds could further be explored for the animal studies. Most of the evaluated compounds showed toxicity class 4, therefore one can say that

TABLE-5
COMPUTATIONAL TOXICOLOGICAL EVALUATION FOR OXADIAZOLES

| Compd. | Predicted toxicity class | Predicted $LD_{50}$ (mg/kg) | Organ toxicity (Hepatotoxicity) | Predicted end points of toxicity | |
|---|---|---|---|---|---|
| | | | | Active for | Inactive for |
| **1** | 4 | 675 | Active | Mutagenicity | Immunotoxicity, cytotoxicity and carcinogenicity |
| **2** | 4 | 1600 | Inactive | Mutagenicity | Immunotoxicity, cytotoxicity and carcinogenicity |
| **3** | 4 | 700 | Active | Mutagenicity and carcinogenicity | Immunotoxicity and cytotoxicity |
| **4** | 4 | 675 | Active | Mutagenicity and carcinogenicity | Immunotoxicity and cytotoxicity |
| **5** | 4 | 675 | Active | Mutagenicity and carcinogenicity | Immunotoxicity and cytotoxicity |
| **6** | 4 | 675 | Inactive | Mutagenicity | Immunotoxicity, cytotoxicity and carcinogenicity |
| **7** | 4 | 675 | Active | Carcinogenicity | Immunotoxicity, mutagenicity and cytotoxicity |
| **8** | 4 | 1600 | Active | Mutagenicity and carcinogenicity | Immunotoxicity and cytotoxicity |
| **9** | 4 | 675 | Active | Mutagenicity | Immunotoxicity, cytotoxicity and carcinogenicity |
| **10** | 4 | 675 | Active | Mutagenicity | Immunotoxicity, cytotoxicity and carcinogenicity |
| **11** | 5 | 3000 | Active | – | Immunotoxicity, mutagenicity, cytotoxicity and carcinogenicity |
| **12** | 5 | 3000 | Active | – | Immunotoxicity, mutagenicity, cytotoxicity and carcinogenicity |
| **13** | 4 | 1000 | Active | Mutagenicity and carcinogenicity | Immunotoxicity and cytotoxicity |
| **14** | 4 | 1000 | Active | Mutagenicity and carcinogenicity | Immunotoxicity and cytotoxicity |
| **15** | 5 | 3000 | Active | – | Immunotoxicity, mutagenicity, cytotoxicity and carcinogenicity |
| **16** | 4 | 1000 | Active | – | Immunotoxicity, mutagenicity, cytotoxicity and carcinogenicity |
| **17** | 4 | 1000 | Active | – | Immunotoxicity, mutagenicity, cytotoxicity and carcinogenicity |
| **18** | 4 | 500 | Active | Mutagenicity and carcinogenicity | Immunotoxicity and cytotoxicity |
| **19** | 4 | 380 | Active | – | Immunotoxicity, mutagenicity, cytotoxicity and carcinogenicity |
| **20** | 4 | 380 | Active | – | Immunotoxicity, mutagenicity, cytotoxicity and carcinogenicity |

they were potentially druggable. All compounds exhibited $LD_{50}$ above 500 mg $kg^{-1}$ which corresponds with toxicity class 4 except compound **11**, **12** and **13**. Among the toxicity classes, class I, II (fetal), whereas class III considered as toxic. However, class IV and class V may be considered as harmful but class VI belongs to non-toxic chemicals.

## Conclusion

The study provides valuable insights into the prospective use of these compounds in targeted cancer therapy. The combination of computational techniques offers a comprehensive understanding of the interaction between 1,3,4-oxadiazoles and the BCL-2 protein, along with an assessment of their pharmacokinetic and toxicological properties. The findings from this study also pave the way for further experimental validation and optimization of lead compounds for the development of targeted and effective therapies for cancer treatment.

## CONFLICT OF INTEREST

The authors declare that there is no conflict of interests regarding the publication of this article.

## REFERENCES


1. J.M. Adams and S. Cory, *Oncogene*, **26**, 1324 (2007); https://doi.org/10.1038/sj.onc.1210220
2. R.J. Youle and A. Strasser, *Nat. Rev. Mol. Cell Biol.*, **9**, 47 (2008); https://doi.org/10.1038/nrm2308
3. D. Hanahan and R.A. Weinberg, *Cell*, **144**, 646 (2011); https://doi.org/10.1016/j.cell.2011.02.013
4. R. Hamdy, S.A. Elseginy, N.I. Ziedan, M. El-Sadek, E. Lashin, A.T. Jones and A.D. Westwell, *Int. J. Mol. Sci.*, **21**, 8980 (2020); https://doi.org/10.3390/ijms21238980
5. A.R. Delbridge and A. Strasser, *Cell Death Differ.*, **22**, 1071 (2015); https://doi.org/10.1038/cdd.2015.50
6. S. Cory and J.M. Adams, *Nat. Rev. Cancer*, **2**, 647 (2002); https://doi.org/10.1038/nrc883
7. F. Marra, A. Gastaldelli, G. Svegliati Baroni, G. Tell and C. Tiribelli, *Trends Mol. Med.*, **14**, 72 (2008); https://doi.org/10.1016/j.molmed.2007.12.003
8. T. Oltersdorf, S.W. Elmore, A.R. Shoemaker, R.C. Armstrong, D.J. Augeri, B.A. Belli, M. Bruncko, T.L. Deckwerth, J. Dinges, P.J. Hajduk, M.K. Joseph, S. Kitada, S.J. Korsmeyer, A.R. Kunzer, A. Letai, C. Li, M.J. Mitten, D.G. Nettesheim, S.C. Ng, P.M. Nimmer, J.M. O'Connor, A. Oleksijew, A.M. Petros, J.C. Reed, S.K. Tahir, C.B. Thompson, K.J. Tomaselli, W. Shen, B. Wang, M.D. Wendt, H. Zhang, S.W. Fesik and S.H. Rosenberg, *Nature*, **435**, 677 (2005); https://doi.org/10.1038/nature03579
9. M. Vogler, *Cell Death Differ.*, **19**, 67 (2012); https://doi.org/10.1038/cdd.2011.158
10. J.C. Reed, *Cell Death Differ.*, **13**, 1378 (2006); https://doi.org/10.1038/sj.cdd.4401975
11. A. Das, M. Sarangi, K. Jangid, V. Kumar, A. Kumar, P.P. Singh, K. Kaur, V. Kumar, S. Chakraborty and V. Jaitak, *J. Biomol. Struct. Dyn.*, (2024); https://doi.org/10.1080/07391102.2023.2256876
12. T.A. Yousef, A.G. Alhamzani, M.M. Abou-Krisha, G. Kanthimathi, M.S. Raghu, K.Y. Kumar, M.K. Prashanth and B.H. Jeon, *Heliyon*, **9**, e13460 (2023); https://doi.org/10.1016/j.heliyon.2023.e13460
13. K. Patil, M. Nemade, A. Bedse, P. Bedse, R. Ranjan, H. Tare and M. Bedse, *Int. J. Drug Deliv. Technol.*, **13**, 966 (2023); https://doi.org/10.25258/ijddt.13.3.31
14. S. Nayak, S.L. Gaonkar, E.A. Musad and A.M.A.L. Dawsar, *J. Saudi Chem. Soc.*, **25**, 101284 (2021); https://doi.org/10.1016/j.jscs.2021.101284
15. Y. Ono, M. Ninomiya, D. Kaneko, A.D. Sonawane, T. Udagawa, K. Tanaka, A. Nishina and M. Koketsu, *Bioorg. Chem.*, **104**, 104245 (2020); https://doi.org/10.1016/j.bioorg.2020.104245
16. A. Tiwari, N.G. Kutty, N. Kumar, A. Chaudhary, P.V. Raj, R. Shenoy, and C. Mallikarjuna Rao, *Cytotechnology*, **68**, 2553 (2016); https://doi.org/10.1007/s10616-016-9979-9
17. A. Daina, O. Michielin and V. Zoete, *J. Chem. Inf. Model.*, **54**, 3284 (2014); https://doi.org/10.1021/ci500467k
18. G. Skoraczyñski, M. Kitlas, B. Miasojedow and A. Gambin, *J. Cheminform.*, **15**, 6 (2023); https://doi.org/10.1186/s13321-023-00678-z
19. Y. Ono, M. Ninomiya, D. Kaneko, A.D. Sonawane, T. Udagawa, K. Tanaka, A. Nishina and M. Koketsu, *Bioorg. Chem.*, **104**, 104245 (2020); https://doi.org/10.1016/j.bioorg.2020.104245
20. M. Soleiman-Beigi, R. Aryan, M. Yousofizadeh and S. Khosravi, *J. Chem.*, **2013**, 476358 (2013); https://doi.org/10.1155/2013/476358
21. A.K. Nagariya, A.K. Meena, S. Kumar, R. Singh, A.K. Yadav and U.S. Niranjan, *J. Pharm. Res.*, **3**, 451 (2010).
22. S. Rochlani, M. Bhatia, S. Rathod, P. Choudhari and R. Dhavale, *Nat. Prod. Res.*, **38**, 891 (2023); https://doi.org/10.1080/14786419.2023.2202398
23. A. Drefahl, *J. Cheminform.*, **3**, 1 (2011); https://doi.org/10.1186/1758-2946-3-1
24. S. Dallakyan and A.J. Olson, *Methods Mol. Biol.*, **1263**, 243 (2015); https://doi.org/10.1007/978-1-4939-2269-7_19
25. A. Daina, O. Michielin and V. Zoete, *Sci. Rep.*, **7**, 42717 (2017); https://doi.org/10.1038/srep42717
26. D.E.V. Pires, T.L. Blundell and D.B. Ascher, *J. Med. Chem.*, **58**, 4066 (2015); https://doi.org/10.1021/acs.jmedchem.5b00104
27. S. Rathod, K. Shinde, J. Porlekar, P. Choudhari, R. Dhavale, D. Mahuli, Y. Tamboli, M. Bhatia, K.P. Haval, A.G. Al-Sehemi and M. Pannipara, *ACS Omega*, **8**, 391 (2023); https://doi.org/10.1021/acsomega.2c04837
28. A.J. Souers, J.D. Leverson, E.R. Boghaert, S.L. Ackler, N.D. Catron, J. Chen, B.D. Dayton, H. Ding, S.H. Enschede, W.J. Fairbrother, D.C.S. Huang, S.G. Hymowitz, S. Jin, S.L. Khaw, P.J. Kovar, L.T. Lam, J. Lee, H.L. Maecker, K.C. Marsh, K.D. Mason, M.J. Mitten, P.M. Nimmer, A. Oleksijew, C.H. Park, C.-M. Park, D.C. Phillips, A.W. Roberts, D. Sampath, J.F. Seymour, M.L. Smith, G.M. Sullivan, S.K. Tahir, C. Tse, M.D. Wendt, Y. Xiao, J.C. Xue, H. Zhang, R.A Humerickhouse, S.H. Rosenberg and S.W. Elmore, *Nat. Med.*, **19**, 202 (2013); https://doi.org/10.1038/nm.3048
29. M. Wiederstein and M.J. Sippl, *Nucleic Acids Res.*, **35(Web Server)**, W407 (2007); https://doi.org/10.1093/nar/gkm290
30. M.J. Sippl, *Proteins*, **17**, 355 (1993); https://doi.org/10.1002/prot.340170404
31. R. Lüthy, J.U. Bowie and D. Eisenberg, *Nature*, **356**, 83 (1992); https://doi.org/10.1038/356083a0
32. A. Singh, R. Kaushik, A. Mishra, A. Shanker and B. Jayaram, *Biochim. Biophys. Acta, Proteins Proteom.*, **1864**, 11 (2016); https://doi.org/10.1016/j.bbapap.2015.10.004
33. R. Gaikwad, S. Rathod and A. Shinde, *Asian J. Pharm. Res.*, **12**, 267 (2022); https://doi.org/10.52711/2231-5691.2022.00043
34. S. Rathod, P. Chavan, D. Mahuli, S. Rochlani, S. Shinde, S. Pawar, P. Choudhari, R. Dhavale, P. Mudalkar and F. Tamboli, *J. Mol. Model.*, **29**, 113 (2023); https://doi.org/10.1007/s00894-023-05521-8
35. V.K. Bagal, S.S. Rathod, M.M. Mulla, S.C. Pawar, P.B. Choudhari, V.T. Pawar and D.V. Mahuli, *Nat. Prod. Res.*, **37**, 4053 (2023); https://doi.org/10.1080/14786419.2023.2165076
36. S. Forli, R. Huey, M.E. Pique, M.F. Sanner, D.S. Goodsell and A.J. Olson, *Nat. Protoc.*, **11**, 905 (2016); https://doi.org/10.1038/nprot.2016.051
37. P. Banerjee, O.A. Eckert, A.K. Schrey and R. Preissner, *Nucleic Acids Res.*, **46(W1)**, W257 (2018); https://doi.org/10.1093/nar/gky318

38. P. Banerjee, F.O. Dehnbostel and R. Preissner, *Front. Chem*., **6**, 362 (2018); https://doi.org/10.3389/fchem.2018.00362
39. M.N. Drwal, P. Banerjee, M. Dunkel, M.R. Wettig and R. Preissner, *Nucleic Acids Res.*, **42(Web Server)**, W53 (2014); https://doi.org/10.1093/nar/gku401
40. R.A. Laskowski, M.W. MacArthur, D.S. Moss and J.M. Thornton, *J. Appl. Cryst.*, **26**, 283 (1993); https://doi.org/10.1107/S0021889892009944
41. R.A. Laskowski, J.A.C. Rullmann, M.W. MacArthur, R. Kaptein and J.M. Thornton, *J. Biomol. NMR*, **8**, 477 (1996); https://doi.org/10.1007/BF00228148
42. R.A. Laskowski, M.W. MacArthur and J.M. Thornton, in eds.: M.G. Rossmann and E. Arnold, PROCHECK: Validation of Protein Structure Coordinates, In: International Tables of Crystallography, Volume F. Crystallography of Biological Macromolecules, Dordrecht, Kluwer Academic Publishers, The Netherlands, pp. 722-725 (2001).
43. A.L. Morris, M.W. MacArthur, E.G. Hutchinson and J.M. Thornton, *Proteins*, **12**, 345 (1992); https://doi.org/10.1002/prot.340120407
44. J.U. Bowie, R. Lüthy and D. Eisenberg, *Science*, **253**, 164 (1991); https://doi.org/10.1126/science.1853201
45. M. Wiederstein and M.J. Sippl, *Nucleic Acids Res.*, **35(Suppl. 2)**, W407 (2007); https://doi.org/10.1093/nar/gkm290
46. D.B. Kitchen, H. Decornez, J.R. Furr and J. Bajorath, *Nat. Rev. Drug Discov.*, **3**, 935 (2004); https://doi.org/10.1038/nrd1549
47. R. Wang and S. Wang, *J. Chem. Inf. Comput. Sci.*, **41**, 1422 (2001); https://doi.org/10.1021/ci010025x